

Comparison of methods for diagnosing marine IC engines based on working medium parameters including exhaust gas specific enthalpy

ARTICLE INFO

The article points out methods currently used to diagnose marine engines in operation. The development of tools and programs for implementing these methods was pointed out. The problem of unsatisfactory measurement susceptibility of marine engines was highlighted. Three methods of parametric diagnosis are presented: measurement of in-cylinder parameters and in exhaust gas duct, numerical simulation due to computer software, and calculations based on the Wibe function. Unfitness states that were analyzed during tests are presented: reduced injection pressure, obstructed intake air duct, and reduced compression ratio. The specific enthalpy of the exhaust gas within one engine cycle was determined as a new diagnostic parameter. As a supplement, thermograms of the engine in various states of inoperability were presented. The results obtained were compared, and a series of conclusions were presented. It was evaluated that numerical simulation is an excellent tool for planning experimental studies. Tests on the engine in operation were found to be the most diagnostically reliable.

Received: 13 September 2024

Revised: 18 October 2024

Accepted: 30 October 2024

Available online: 6 November 2024

Key words: *marine diesel engine, parametric diagnostics, Wibe heat release function, indicator diagram, specific enthalpy of exhaust gas, thermograms of engine*

This is an open access article under the CC BY license (<http://creativecommons.org/licenses/by/4.0/>)

1. Introduction

Three functional system maintenance strategies are currently applied to marine engines, depending on the operating conditions of the system under analysis: PPM (Planned Preventive Maintenance), CBM (Condition Based Maintenance) and FFF (For the First Failure) [9]. Depending on the strategy used, the operator chooses the appropriate diagnostic test method based on the condition of the marine engine's equipment with standard control and measurement devices. Based on these devices, he has access to the engine's control parameters, called a "set of parameters measured routinely" [38]. Some of these are a minimum set, relevant to the safety of the vessel, and are defined by the regulations of classification societies [4–6]. However, it is considered that the set of these parameters is insufficient for reliable diagnostics of the functional systems of the ship's engine covered by the CBM operation strategy. More complete data can be obtained during periodic surveys, during which it is possible to supplement the data held with parameters additionally recorded.

Early detection of damage to engine functional systems can be guaranteed through the widespread use of diagnostic equipment and systems on ships [26, 35, 38]. In addition to these systems, no less important is the implementation of new diagnostic techniques that allow more in-depth information about the technical condition based on additionally recorded parameters. Among the methods commonly used and also included in the above systems are several. A lot of important diagnostic information can be obtained during engine indicating [28, 39]. The second method to assess the technical condition is the analysis of exhaust gas parameters. While exhaust gas pressure measurement is not always performed, temperature measurement is required by classification societies, especially if a system equipped with a utilization boiler or turbocharger is involved. A lot of

diagnostic information is also contributed by measuring vibrations generated, for example, by the injector [30]. For a similar purpose, the measurement of noise in the background of an indicator diagram, proposed by Prof. Verbanets, can be used [34]. Environmental pollution has been an important aspect for many years. Analyzing the composition of the exhaust gas is a well-developed method and allows, in addition to protecting the marine environment, to diagnose engine malfunctions [7, 13]. Thermal imaging could be mentioned as the last way to diagnose a marine engine [17]. The temperature distribution of the engine's working surfaces makes it possible, among other things, to determine heat loss to the environment, to determine the balance and efficiency of the engine (Sankey diagram), and also to diagnose malfunctions that result in an increase in engine operating temperature.

Many of the mentioned diagnostic methods have developed over the years resulting in greater accuracy of measurements and precision of diagnosis. Software is being introduced into widespread use, which, on the basis of very accurate simulation models, determines the waveforms of control and diagnostic parameters depending on changes in the functional systems of the engine. This is a tool carrying support before proceeding to experimental tests on the real object, among other things, to select diagnostic parameters that will respond most strongly to the expected malfunction. In parallel, the technology of measurement tools is developing: pressure sensors, exhaust gas composition analyzers, indicators, vibration sensors, or thermal imaging cameras allow increasingly accurate measurements and more accurate diagnosis. Standard measurements, based on measuring the average temperature of exhaust gases of engines in operation, are now very well developed. However, there is an information gap in the diagnostic use of measurements of dynamic changes in exhaust gas temperature, even

though temperature sensors with very small time constants are used in other industries [8].

Not all marine engines in operation today are equipped with indicator valves, and it is not always possible to measure exhaust gas pressure. While measuring the temperature inside the combustion chamber poses problems for diagnosticians if only because of the durability of the temperature sensors, measuring the rapidly varying exhaust gas temperature by adapting an existing thermocouple can give much more diagnostic information within a single engine cycle, for example, based on the specific enthalpy of the exhaust gas [23].

2. Description of considered diagnostic methods

This article analyzes the results obtained by the following methods:

- by numerical simulation of thermodynamic processes occurring in the combustion chamber using the Diesel-RK program
- in the results of measurements of diagnostic parameters on the laboratory bench of the IC engine Farymann
- by calculating the engine's operating parameters based on the values obtained during the measurements, according to thermodynamic relationships, mainly the Wibe function
- thermography of the surface of the test engine as a supplement to the above data.

Computer numerical simulation of the processes carried out in the laboratory engine was done using the Diesel-RK program [20]. The Diesel-RK computer program is designed to simulate and optimize the working processes of two-stroke and four-stroke engines for all types of supercharging and for the various fuels used. The software's capabilities allow the input of design data (such as piston diameter and stroke, combustion chamber volume, injection system parameters and timing) and operating data (such as crankshaft rotational speed, EGR value, feed air parameters, injection delay or fuel type) of any engine. During the numerical simulation of the processes, the design and operating data of the laboratory engine and the elementary composition of the MGO (Marine Gas Oil) feed fuel used during the experimental tests were entered. The program also allowed the introduction of partial unfitness states, which made it possible to select and analyze diagnostic parameters.

In the next step, tests were performed on a laboratory bench of a four-stroke, single-cylinder, naturally aspirated IC engine Farymann Diesel type D10, whose receiver is a DC generator, which in turn powers a heater – Fig. 1 [12]. The nominal parameters are: $P = 6 \text{ kW}$, $n = 1500 \text{ min}^{-1}$, $M = 38 \text{ Nm}$, $d_{\text{cyl}} = 90 \text{ mm}$, $S_{\text{cyl}} = 120 \text{ mm}$, $CR = 22:1$, displacement 765 cm^3 . During laboratory tests, MGO fuel ($C = 0.8626$, $H = 0.111$) was burned, $n = 1444 \text{ min}^{-1}$ was maintained, and engine power was at 1.2 kW. The parameters recorded were derived from the control susceptibility of the engine and the available measuring instruments. Intra-cylinder pressure and exhaust gas duct pressure were recorded using Optrand optical sensors [18]. Rapidly varying temperature in the exhaust gas duct was measured using a K-type thermocouple (NiCr-Ni) with an outer diameter of the sheath of 0.5 mm, with a welded joint, with a time con-

stant of 65 ms from Termoprecyzja company – Fig. 2 [24, 33]. The composition of the exhaust gas and the value of the excess air ratio were also recorded using a KIGAZ 300PRO electrochemical analyzer – Fig. 3 [1, 10].

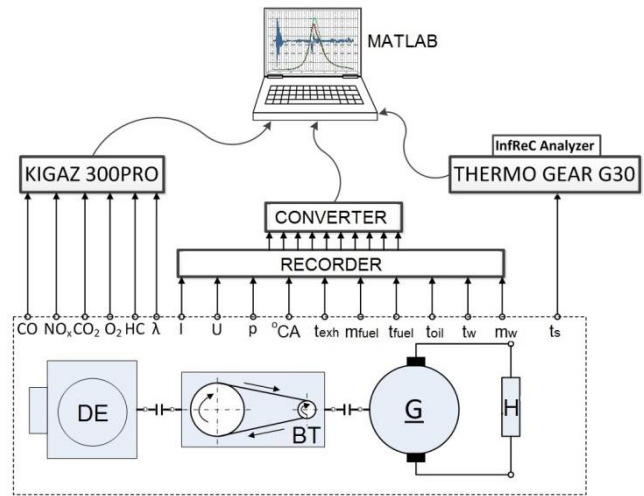


Fig. 1. Schematics of the test stand with the measurement signals recording and processing system: DE – Farymann D10 diesel engine; BT – belt transmission; G – direct current generator; H – system of heaters



Fig. 2. Photo and cross-section of a type K thermocouple used in rapidly variable measurements



Fig. 3. View of the KIGAZ 300PRO flue gas analyzer used in laboratory tests

The calculations were based on thermodynamic relationships between engine operating parameters [19, 31, 40]. Relationship (1) determines the average temperature of the medium in the engine cylinder from the moment the intake valve closes to the moment the exhaust valve opens, so it follows that as the pressure of the operating medium in-

creases, its temperature will also increase. Thus, the generation and exchange of heat between the working medium and the structural elements that make up the combustion chamber are not taken into account in this relationship [2, 41]:

$$T(\alpha) = \frac{p_f(\alpha) \cdot V_f(\alpha)}{m_f R_f}, K \quad (1)$$

where: p_f – pressure in the engine cylinder, V_f – volume of the fluid in the cylinder, m_f – mass of the fluid charge in the cylinder, R_f – individual gas constant of the working fluid.

Based on the measured excess air ratio, fuel composition, geometric parameters of the engine, the temperature of the working medium in the cylinder was calculated based on the Wibe formula to determine the amount of heat released during the combustion process [16, 19, 21, 27, 29]:

$$x = 1 - e^{-a \cdot y^{m+1}} \quad (2)$$

where: m – parameter characterizing the dynamics of the course of heat release (for IC engines 0.1–1.0), a – coefficient taking into account the degree of combustion of the total fuel dose in 1 cycle (for 99.9% of fuel burned is – 6.908), x – amount of heat release, $y = t/t_c$, where t – time of combustion of the fuel dose from the beginning of injection to the moment considered, t_c – total time of combustion of the fuel dose in 1 cycle.

Looking for a meaningful calculation of the temperature of the working fluid in the cylinder, it is necessary to accurately determine the pressure variation from the indicator diagram. Even under established engine operating conditions, indicator diagrams for successive cycles differ from each other. This is mainly due to the uniqueness in successive operating cycles of the parameters of the injected fuel spray, the filling of the cylinder with a fresh load and the amount of residual exhaust gas remaining in the cylinder from the previous operating cycle, and hence the uniqueness of the combustion process. Thus, a waveform averaged over dozens of cycles should be used to determine the working gas temperature [36].

The study and calculation of the courses of variation of the temperature of exhaust gases leaving the engine cylinders in the range of the duration of one cycle of operation provides the possibility of a direct qualitative and quantitative assessment of the specific enthalpy of the exhaust gas stream. The value of this calculation parameter is determined by integrating the course of the rapidly varying temperature of the exhaust gas within the limits defined by the values of the angle of rotation of the engine crankshaft for one duty cycle, with a known value of the specific heat of the exhaust gas at constant pressure, calculated from stoichiometric equations in the range of temperatures prevailing in the control section of the exhaust gas outlet channel [37]:

$$h_{exh} = \int_0^{720} c_{exh}(T_{exh}) \cdot T_{exh} d\alpha_{CA}, J/kg \quad (4)$$

where: h_{exh} – specific enthalpy of the exhaust gas stream, average within one engine cycle, J/kg, $c_{exh}(T_{exh})$ – average specific heat of the exhaust gas at constant pressure, kJ/kg·K, T_{exh} – exhaust gas temperature recorded within

one engine cycle, K , α_{CA} – value of engine crankshaft rotation angle, CA.

The value of the average specific heat of exhaust gas was determined on the basis of fuel composition and excess air ratio measurements [37].

In the case of the analysis of rapidly varying exhaust gas temperature, the obtained signal was subjected to a two-step mathematical treatment. In the first step, the disturbances were removed from the measurement network using a Savitzky-Golay filter in Matlab software [14]. In the second step, an amplitude-phase correction was made to obtain the real exhaust gas temperature waveform. The phase shift of the temperature variation recorded by the thermocouple in relation to the variation of the exhaust gas temperature is [37]:

$$\varphi = -\arctg(\omega \cdot \tau') \quad (5)$$

Meanwhile, the amplitude of the temperature variation recorded by the thermocouple is:

$$t_{aexh} = t_a \cdot \sqrt{1 + \omega^2 \cdot \tau'^2} \quad (6)$$

According to the above, the real temperature of the exhaust gas is:

$$t = t_{0exh} + t_a \cdot \sin(\omega \cdot \tau + \varphi) \quad (7)$$

where: τ – time, t – real temperature, t_a – amplitude of temperature change recorded by thermocouple, t_{aexh} – amplitude of temperature change of exhaust gas, t_{0exh} – initial temperature of exhaust gas, τ' – time constant, ω – pulsation frequency of temperature change.

In this way, the response of the thermocouple to a sinusoidal forcing of the exhaust gas temperature was obtained. The temperature signal in the exhaust gas channel thus prepared was analyzed.

In addition, thermograms of the working surfaces of the engine and the exhaust gas duct were recorded. An NEC Thermo Gear G30 camera and InfReC Analyzer NS9500 LT software from the manufacturer of the thermal imaging camera were used for this purpose [32].

3. Analyzed states of unfitness

Both during the numerical simulation in the Diesel-RK program and during the tests, 4 technical states of the Farymann laboratory engine were considered (Fig. 4):

- 1) state of full operational fitness (reference) – the results obtained in this state allowed a comparative evaluation of the introduced states of partial fitness (simulated) on the course of thermal-fluid processes
- 2) state of partial operational suitability, with simulated reduced compression ratio (increased combustion chamber volume)
- 3) state of partial operational fitness, with simulated relaxation of the injector spring (reduced injector opening pressure)
- 4) state of partial operational suitability, with simulated loss of patency of the air intake duct (tightened control valve in the duct).

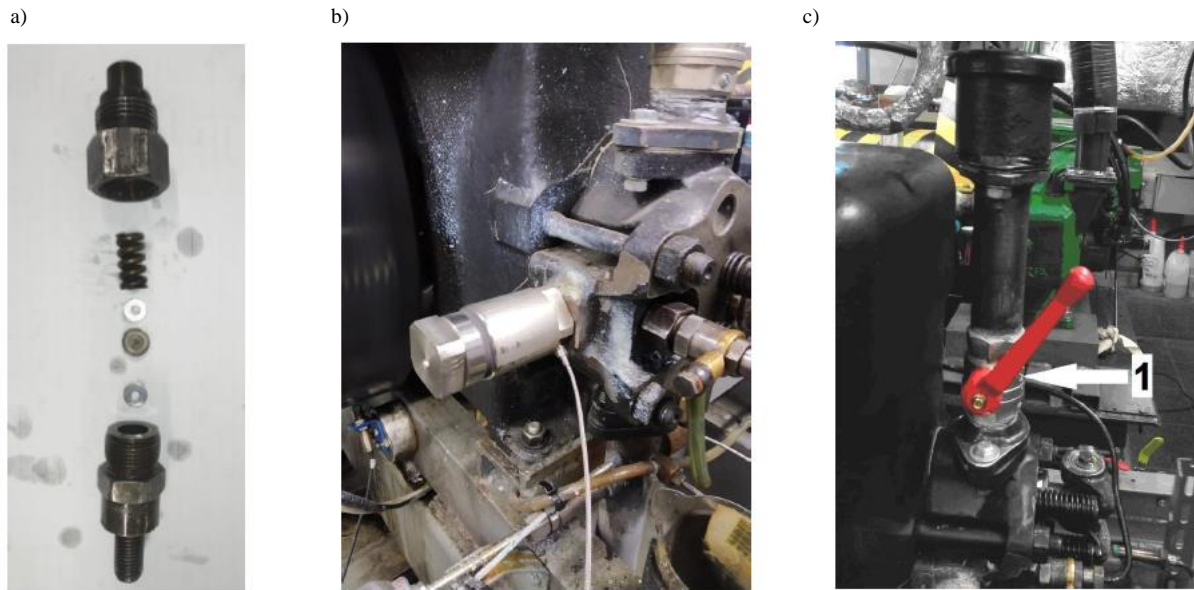


Fig. 4. View of the structural elements of the injector used during the tests, including the replaceable (adjusting) shims under the injector spring (a), the structural element adjusting the combustion chamber volume (b), view of the inlet air duct feeding the engine (c); 1 – air control valve

The state of full serviceability applies to the Farymann laboratory engine, which initially served as an auxiliary engine in the power plant of a fishing vessel. After dismantling, it was adapted to a laboratory bench, where it was subjected to cyclic renovations [11, 12].

In the engine's next state, changes were made to the structural parameter of combustion chamber volume. This was reflected in reduced values of the engine's compression ratio, which is a fairly common condition of its operational unfitness [9]. The reference value of the compression ratio for the tested engine is $CR_{REF} = 22:1$, while the reduced value was $21:1$. The small range of the introduced changes in CR is due to the high sensitivity of the test engine to even the smallest changes in the value of this structural parameter. The reduction of the compression ratio was realized by using an additional structural element to increase the volume of the combustion chamber – Fig. 4b.

In the third condition, the tension of the injector spring was changed by the appropriate selection of shims. This simulated its relaxation lowering the opening pressure of the injector. Lowering the injector opening pressure p_{inj} from 12 MPa to 10 MPa simulated a failure of the fuel injection system involving too early injection of fuel into the combustion chamber – Fig. 4a.

In the last step, the value of the active cross-sectional area of the intake air duct A_{in} was changed relative to the reference state, understood as the full opening of the air control valve, which simulated the loss of patency of the filter baffle – Fig. 4c.

The above states were also (prior to the active experiment) entered into the Diesel-RK simulation program, assuming the design capabilities of the test engine. Unfortunately, the program does not allow to take into account the conditions in the laboratory during the test or the condition of the engine. However, the evaluation of the choice of diagnostic parameters was not quantitative, so such a model was considered sufficient.

4. Obtained results of research, simulations and calculations

4.1. Numerical simulation in the Diesel-RK program

The engine cycle was simulated for the reference condition and for reduced compression ratios (from $22:1$ to $21:1$), injector opening pressures (20 bar less than in the reference state) and a reduced intake air duct cross-sectional area (50% less than the reference condition) to illustrate the most common damage occurring in IC marine engines. The focus was most on the following output parameters, calculated in the Diesel-RK program:

- temperature and pressure of the working fluid in the cylinder (T_{cyl} and p_{cyl})
- exhaust gas temperature and pressure in the exhaust duct (T_{exh} and p_{exh}).

As shown in Fig. 5a, the simulated unfitness states affected the value of the in-cylinder pressure. In the case of a reduced value for the cross-sectional area of the intake air duct A_{in} , no significant difference is apparent (the red line overlaps with the blue line). However, the reduced injection pressure p_{inj} results in a drop in maximum pressure of around 2.2 bar. The biggest difference can be seen in the case of reduced compression ratio CR already at the compression phase, then combustion, where the difference in maximum pressure is about 4.68 bar.

For the temperature of the medium inside the combustion chamber (Fig. 5b), the most significant difference is seen in the case of reduced p_{inj} (about 24.6 K).

Analysing the exhaust gas pressure in the exhaust duct (Fig. 5c), the blue line coincides with the red line (reference condition with A_{in}), which can be interpreted as no influence of A_{in} on this parameter. On the other hand, the purple line coincides with the green line (p_{inj} and CR), which may mean that these two unfitness states affect this diagnostic parameter similarly. The maximum pressure increases by approximately 0.014 bar when dealing with reduced p_{inj} or CR relative to the reference condition.

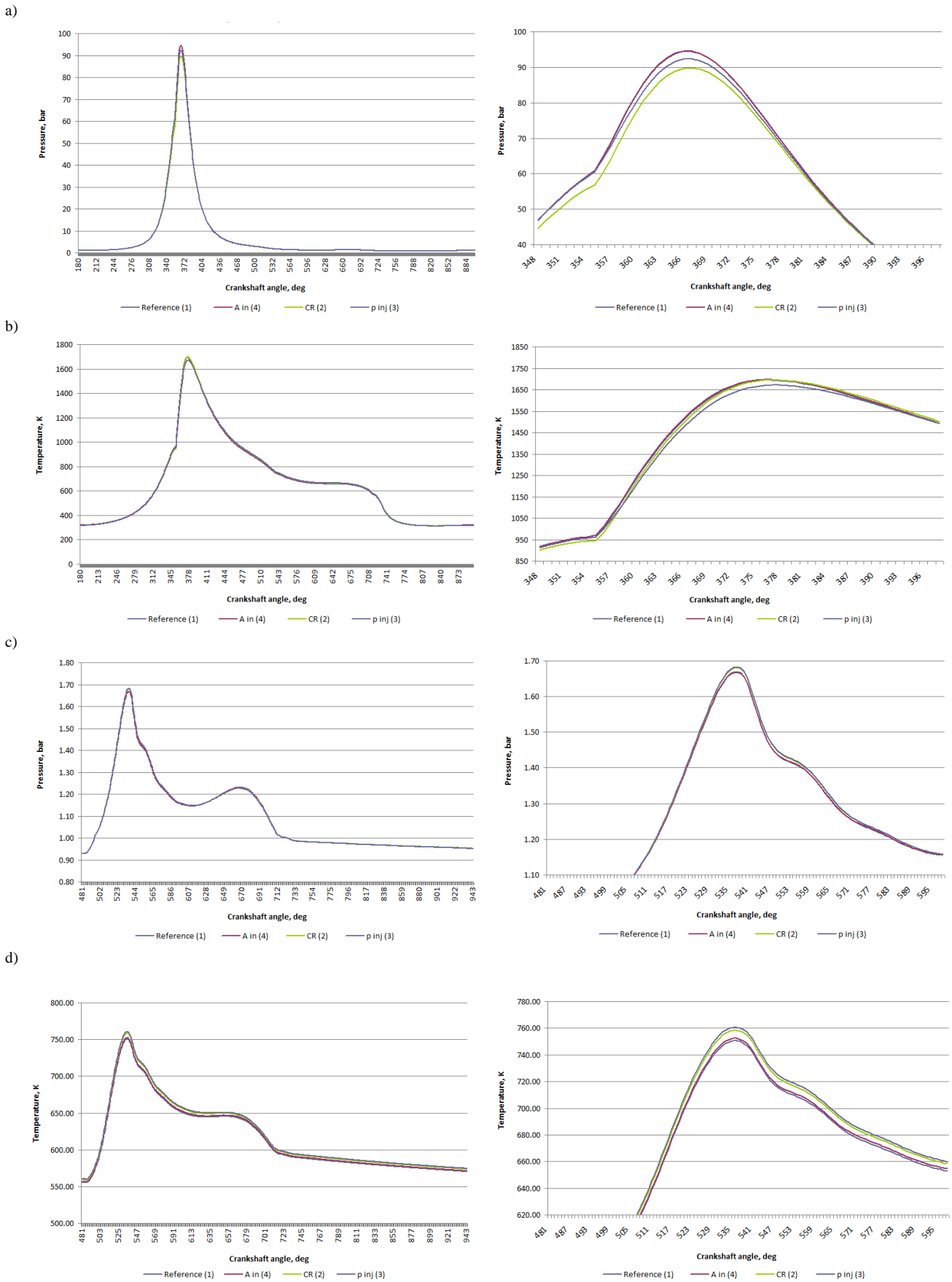


Fig. 5. Fluctuations in the in-cylinder working fluid parameters: pressure p_{cyl} (a) and temperature T_{cyl} (b) and in the exhaust gas duct: pressure p_{exh} (c) and temperature T_{exh} (d); the figures on the left show the parameter fluctuations as a function of crankshaft rotation angle, while on the right the areas of greatest variation have been enlarged

A similar situation occurs for the exhaust gas temperature (Fig. 5d). Reduced A_{in} has no significant effect on this parameter, while reduced p_{inj} and CR result in a temperature increase of approximately 8.5 K.

Analysing the above graphs, it was concluded that the simulated selected unfitness states have a significant effect on the value of the analysed parameters, particularly in the combustion phase (when the maximum values of the analysed parameters occur). It was therefore considered that the analysis of p_{cyl} , p_{exh} , T_{cyl} and T_{exh} as diagnostic parameters during laboratory tests would be meaningful.

4.2. Measurement results on the laboratory bench

The tests were carried out on the laboratory bench of a Farymann Diesel engine type D10, for 4 operating states: reference and 3 unfitness, the same as for the simulations in the Diesel-RK program. Representative waveforms are shown in Fig. 6 and described below.

The waveforms shown in Fig. 6 were created by measurements on the laboratory bench. Everywhere, the TDC signal from the inductive sensor used was taken as the origin of the decimal axis. The sensor itself can contribute small shifts (distortions) to the signal, but the information extracted from it was for illustrative purposes only and was not considered for accurate quantitative analyses.

As with the simulations, it is shown in Fig. 6a that the intra-cylinder pressure value decreased (by about 990 kPa) as a result of the reduced CR and p_{inj} values. The p_{cyl} waveform for reduced A_{in} coincides over almost the entire range

with the reference condition, but a difference in the maximum value of this parameter in the form of a slight decrease (about 877 kPa) is apparent. The reason for the shift in the maximum of the waveform was considered to be an inaccuracy of the TDC sensor indications. Measurement of the in-cylinder T_{cyl} temperature was not possible due to the design capabilities and test susceptibility of the laboratory engine.

The measurement of the exhaust gas duct pressure took place at the same location as the temperature measurement and also indicated a relationship analogous to that of the simulation. Reduced CR and p_{inj} values resulted in increased p_{exh} values of approximately 1470 Pa on CR and 430 Pa on p_{inj} , respectively, on average – Fig. 6b.

In the case of the exhaust gas temperature varying rapidly within one cycle, the measurement was made at a distance of 15 cm from the outlet valve plug, using a thermocouple mounted in a straight section of the duct. The waveform shown in Fig. 6c is recorded and free of noise only with filtering to remove noise from the measurement network. The effect of reduced A_{in} on the T_{exh} value is evident: a decrease in value of about 30 K. It is also noticeable that the fluctuations of the waveforms increase with the introduced in-service unfitness states, especially for CR. In the case of the actual temperature of the exhaust gas, obtained by amplitude-phase correction, an increase in the dynamics (higher fluctuations) of the waveforms for unfitness states relative to the reference state is also apparent – Fig. 6d.

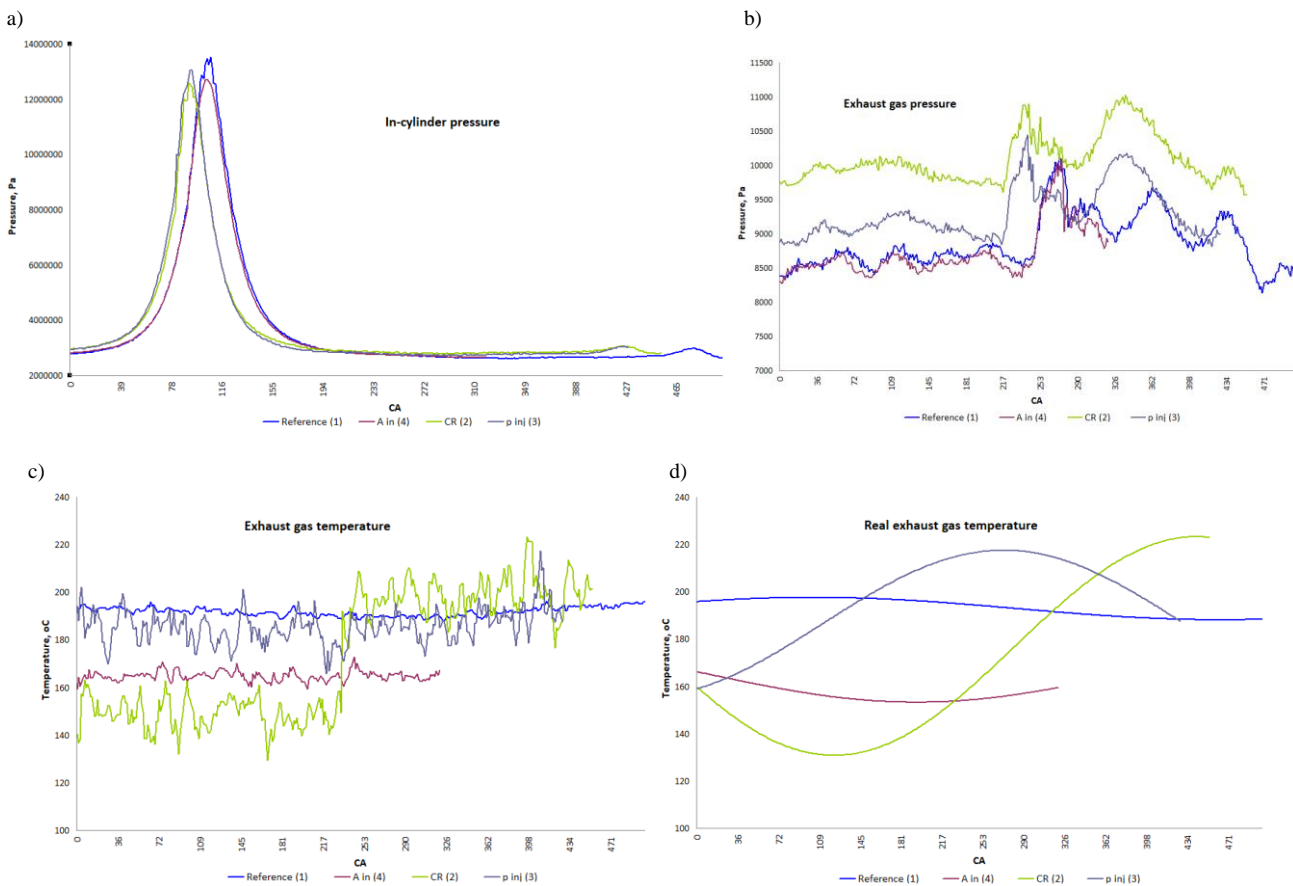


Fig. 6. Fluctuation curves of the measured parameters of the working medium: intra-cylinder pressure (a), pressure in the exhaust gas duct (b), recorded exhaust gas temperature (c), real exhaust gas temperature (d)

4.3. Results of the calculations of the operational cycle parameters

Based on Wibe's formula (2), a script was created in Matlab 2023a to determine, among other things, the values of in-cylinder pressure and temperature – Fig. 7. The most important input parameters for the calculations included: the geometrical dimensions of the laboratory engine, its compression ratio, crankshaft rotational speed during testing, composition and calorific value of the fuel used during research, as well as the exponents adopted by iterative simulations: compression, expansion, and the coefficient m describing the dynamics of heat release during combustion in the IC engine. The proposed script allowed changes to be made to the values of compression ratio and pressure reduction during intake, in addition to the reference condition.

Analysing the in-cylinder pressure and temperature variation waveforms obtained from the calculations, several conclusions can be drawn. For all analysed 3 states, a shift of the maximum temperature value in relation to the maximum pressure value by 10–12°CA is visible, which is in accordance with common knowledge [25]. A similar relationship was obtained in Diesel-RK, which was not mentioned earlier. Comparing the maximum p_{cyl} values, it is apparent that for the reduced compression ratio (Fig. 7c) it increased by 4.8% relative to the reference condition (Fig. 7a). The maximum T_{cyl} temperature (Fig. 7d) also increased by 15.2% relative to the reference condition (Fig. 7b). In the case of the reduced intake pressure drop by half, it was the intake air pressure value that was adjusted, not the cross-sectional area of the intake air duct, which was the case during the simulation in the Diesel-RK program and during the tests on the laboratory bench. This is, therefore, an input parameter that only partially coincides with A_{in} . In the case of p_{cyl} pressure (Fig. 7e), a significant drop was recorded: by 47% relative to the reference condition (Fig. 7a). On the other hand, the temperature T_{cyl} (Fig. 7f) increased by 9.6% compared to the reference condition (Fig. 7b).

According to relationship (4), the specific enthalpy of the exhaust gas was calculated for each laboratory engine condition taken into account. The specific enthalpy values of the exhaust gas for the temperature measured in the exhaust duct, shown in Fig. 8, are the average of 90 consecutive cycles, for each measurement. The adoption of 90 duty cycles as representative and subject to synchronous averaging resulted, among other things, from an analysis of the data and technical capabilities of commercially available cylinder pressure analyzers [3, 22]. Based on the above data, therefore, roughly twice the number of cycles analysed in terms of their averaging was assumed, considering this to be a sufficient value for the elimination (reduction) of noise, which in this case reduced the standard deviation of noise by about 9-times [15]. It was also taken into account that there was an increase in file size resulting from the amount of data being subjected to the relevant calculations or statistical analyses with more engine cycles, which brought greater demands on the software and computer. The enthalpy values were determined for real waveforms, and subjected to signal processing to remove noise from the

measurement network and subsequent amplitude-phase correction (Fig. 6d).

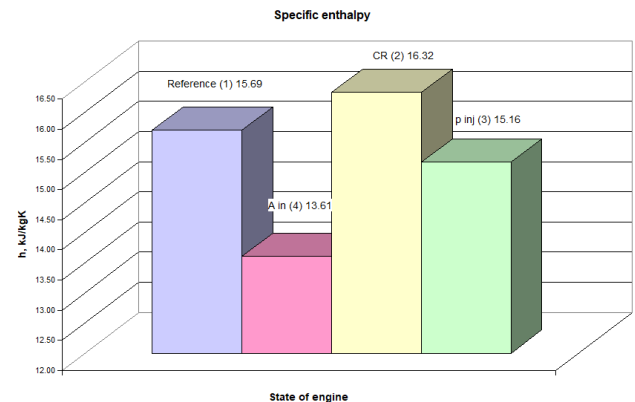


Fig. 8. Exhaust gas specific enthalpy values for the real exhaust gas temperature course, for four operating states of the test engine

As can be seen in Fig. 8, the reduction in the intake air flow field resulted in a reduction in the specific enthalpy value h for one engine cycle of approximately 2 kJ/kg·K (13%). This is primarily due to a reduction in exhaust gas temperature for a smaller volume of combustion air. In contrast, the reduced compression ratio resulted in a slight increase in h (by about 0.63 kJ/kg·K, 4%), which may be due to the higher fluctuations in the mileage for this condition. In the case of reduced fuel injection pressure, the enthalpy h decreased its value by about 0.53 kJ/kg·K (3.4%), so this effect can be considered significant. The statistical analysis carried out, based on the analysis of variance, showed a statistically significant effect only for A_{in} . This means that damage to the air intake system must be inferred from the specific enthalpy of the exhaust gas within one operating cycle.

4.4. Thermography of engine surfaces

Thermography of the engine side surfaces was carried out to determine the effect of the introduced inoperative states on the temperature at the characteristic measurement points as a supplement to the diagnostic information (Fig. 9). The temperature values for the same engine load were compared at the following points: at the initial section of the exhaust gas duct, at the cylinder head, at the top of the engine hull, at the top of the water jacket of the cylinder liner and at the cooling water tank. An advantage of the laboratory engine is the simplified design of the fuel supply, lubrication and cooling systems, which is important for balancing the processes within it. The solution of an integrated cooling water tank increases the autonomy of the engine as a laboratory bench. Analysing the representative thermograms shown in Fig. 9, it can be seen that for all states of unfitness, a decrease in temperature was recorded at almost all measuring points of the engine surface relative to those for the reference condition. In all cases, this was a decrease of 0.6–20 K. The exception is point c (upper part of the engine hull), where for reduced A_{in} and p_{inj} the temperature recorded a slight increase (4–5 K).

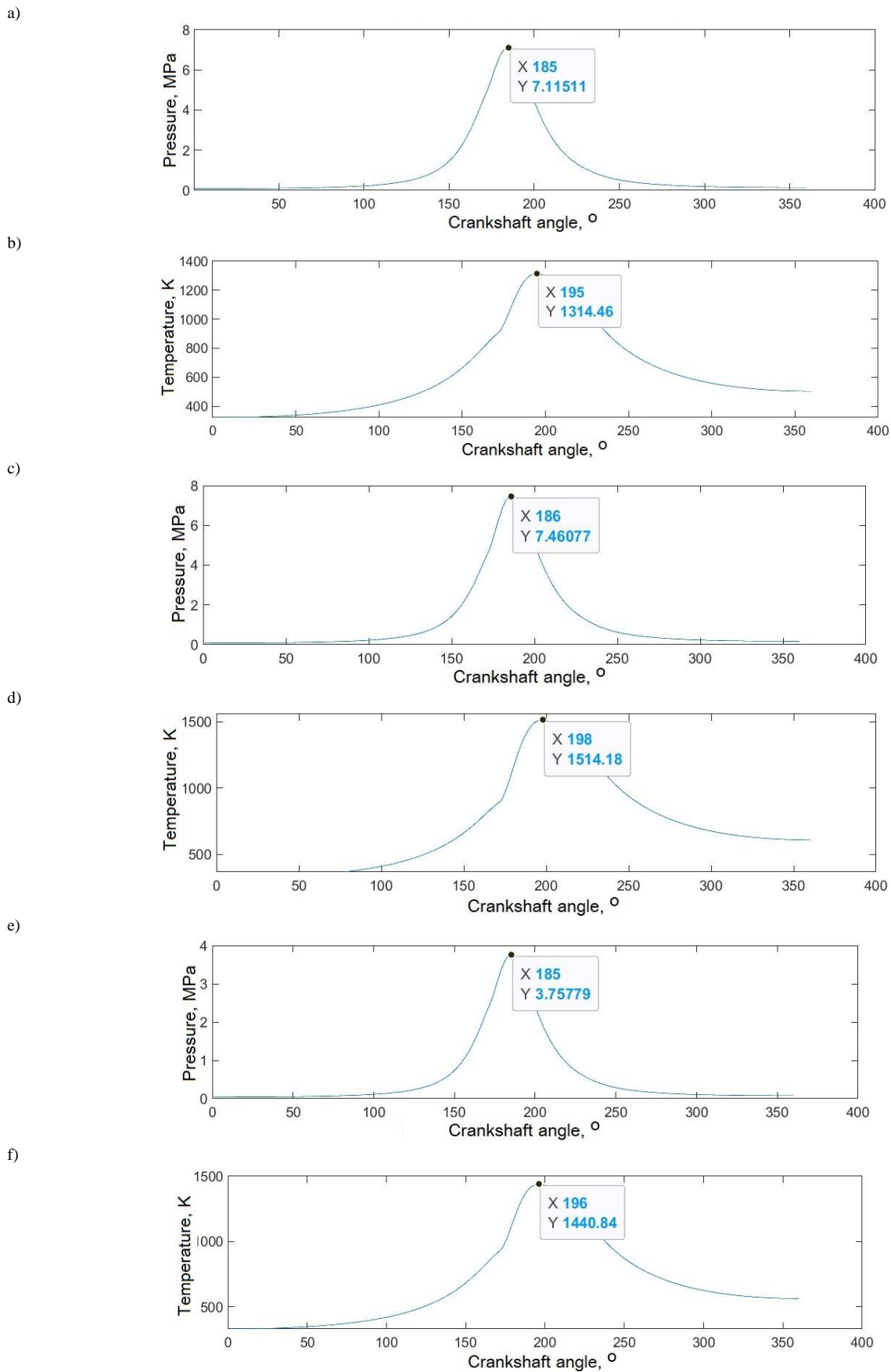


Fig. 7. The variation curves of the temperature of the working medium in the cylinder as a function of the angle of rotation of the crankshaft, together with the marked maximum values of the parameters: pressure (a) and temperature (b) in the reference state, pressure (c) and temperature (d) for reduced compression ratio, pressure (e) and temperature (f) for throttled intake air; TDC = 180 CA

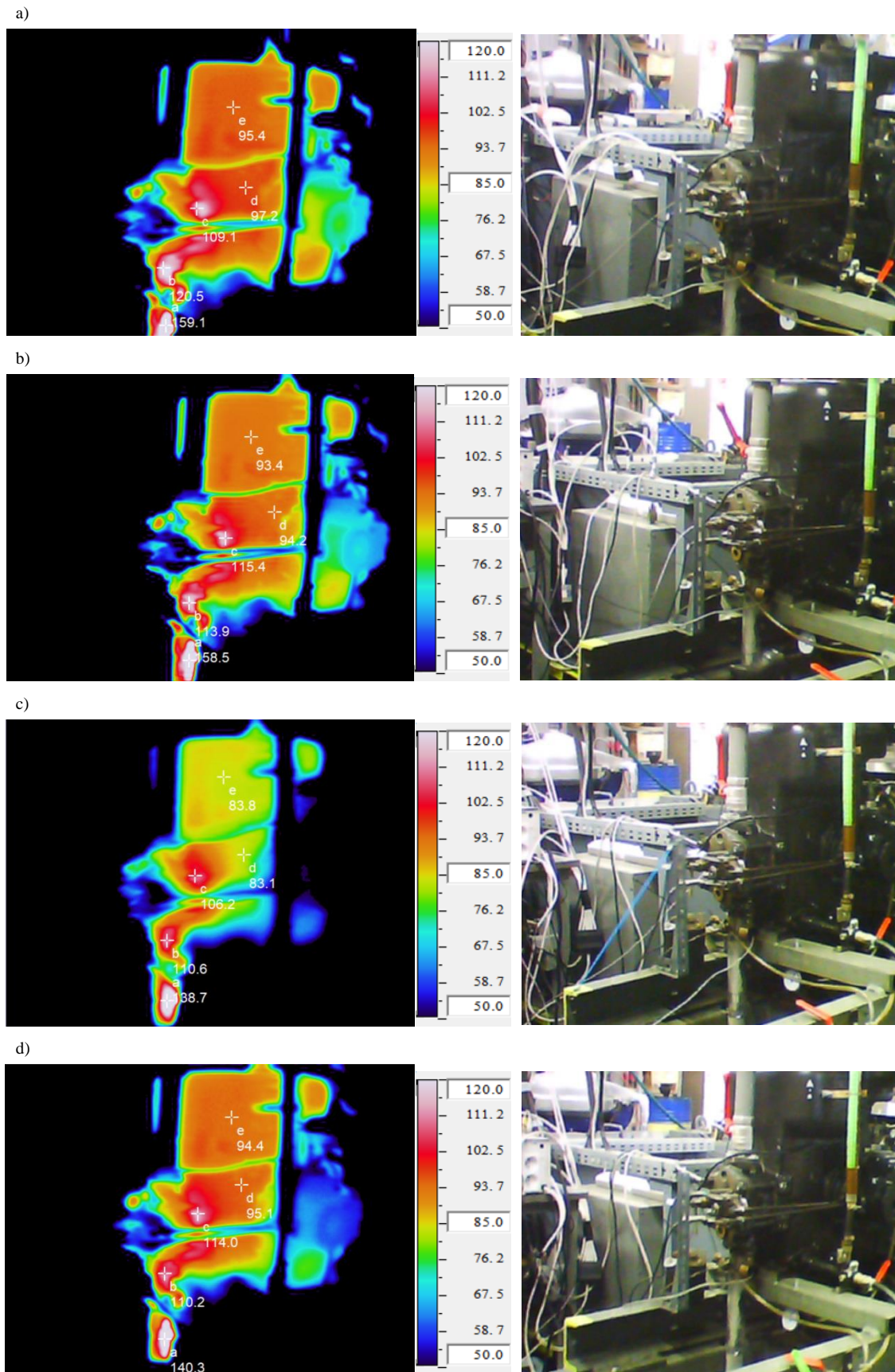


Fig. 9. Thermograms of the Farymann Diesel test engine for four operating states: a) reference state, b) reduced supply air condition, c) reduced compression ratio, d) reduced injection pressure; points: a – beginning of the exhaust gas duct, b – cylinder head, c – upper part of the engine hull, d – top of the cylinder liner water jacket, e – cooling water tank

5. Conclusions

Summarizing the research, calculations and analyses carried out, the following conclusions were drawn:

- numerical simulation of engine processes gives valuable information on the selection of appropriate diagnostic parameters and, at low cost, is sufficient for this purpose and for preliminary diagnosis
- simulation programs do not reflect the actual test conditions, so evaluation based on their results can only be qualitative, not quantitative
- in the case of experimental testing, it is necessary to select appropriate diagnostic parameters and to measure them at high sampling rates – rapidly variable measurement gives more diagnostic information than averaged measurement
- during tests, the engine should be loaded as much as possible and the values of the diagnostic parameters should be analysed in the areas of their maximum occurrence – this is when the differences are greatest and the diagnostic information is, therefore most reliable
- when it is not possible to measure all the diagnostic parameters, it is possible to determine the remaining parameters by calculating the heat release in the cylinder; under certain conditions, this is a sufficient method [41]

- if cylinder indexing is not possible, measurement of exhaust gas temperature is a valuable diagnostic parameter
- the rapidly variable exhaust gas temperature signal should be subjected to the appropriate proposed mathematical treatment – Savitzky-Golay filtering and amplitude-phase correction in order for the results to be meaningful
- comparison of the results obtained by the three methods mentioned above is possible only to a certain extent; this is due, among other things, to different input data, different calculation algorithms or ways of processing test data, or conditions prevailing during the test which cannot be modeled in a computer program
- an important supplement to parametric diagnostics are thermograms of the engine surface, which provide information about the amount of heat released by the machine
- development of the proposed diagnostic method would allow the determination of the heat balance of the engine – a Sankey diagram, which brings information about the thermal efficiency of the engine in the analysed operating condition [12]
- the proposed method of determining the specific enthalpy of the exhaust gas can be applied to the diagnostics of marine engines in service after appropriate adaptation of the existing thermocouples [25].

Nomenclature

A_{in} intake air duct area
 CR compression ratio
 EGR exhaust gas recirculation
 h specific enthalpy
 IC internal combustion
 MGO marine gas oil

p_{cyl} in-cylinder pressure
 p_{exh} exhaust gas pressure
 p_{inj} opening pressure of injector
 T_{cyl} in-cylinder temperature, K
 T_{exh} exhaust gas temperature
 TDC top dead center

Bibliography

- [1] Exhaust gas analyzer data. greentechtools.com (accessed on 3.07.2024).
- [2] Hunicz J. Modelowanie silników spalinowych (Modeling of internal combustion engines). Lublin University of Technology Publishing House, Lublin 2014.
- [3] Information on exhaust gas analysis composition devices. iconresearch.co.uk/diesel-engine-analysis/doctor-portable/ (accessed on 11.07.2024).
- [4] International Association of Classification Societies, Requirements Concerning Machinery Installations. M35: Alarms, remote indications and safeguards for main reciprocating I.C. engines installed in unattended machinery spaces: 2016.
- [5] International Association of Classification Societies, Requirements Concerning Machinery Installations. M36: Alarms and safeguards for auxiliary reciprocating I.C. engines driving generators in unattended machinery spaces: 2016.
- [6] International Association of Classification Societies, Requirements Concerning Machinery Installations. M73: Turbochargers: 2016.
- [7] Kęska A. The actual toxicity of engine exhaust gases emitted from vehicles: the development and perspectives of biological and chemical measurement methods. ACS Omega. 2023;8(28):24718-24726. <https://doi.org/10.1021/acsomega.3c02171>
- [8] Korczewski Z, Puzdrowska P. Analytical method of determining dynamic properties of thermocouples used in measurements of quick – changing temperatures of exhaust gases in marine diesel engines. Combustion Engines. 2015;162(3): 300-306.
- [9] Korczewski Z. Diagnostyka eksploatacyjna okrętowych silników spalinowych – tokowych i turbinowych. Wybrane zagadnienia (Operational diagnostics of marine internal combustion engines – piston and turbine engines. Selected issues). Gdańsk University of Technology Publishing House. Gdańsk 2017.
- [10] Korczewski Z. Energy and emission quality ranking of newly produced low-sulphur marine fuels. Pol Marit Res. 2022;29:77-87. <https://doi.org/10.2478/pomr-2022-0045>
- [11] Korczewski Z, Rudnicki J, Piechowski L, Cenian A. Investigations of a D10 laboratory Farymann Diesel engine by means of a Langmuir probe. Combustion Engines. 2013;153(2):75-82. <https://doi.org/10.19206/CE-117004>
- [12] Korczewski Z. Metodyka testowania paliw żeglugowych w rzeczywistych warunkach pracy silnika o zapłonie samoczynnym (in Polish). Gdansk University of Technology Publishing House. Gdansk 2022.
- [13] Kowalski J. Concept of the multidimensional diagnostic tool based on exhaust gas composition for marine engines. Appl Eng. 2015;150:1-8. <https://doi.org/10.1016/j.apenergy.2015.04.013>

- [14] Luo J, Ying K, Bai J. Savitzky-Golay smoothing and differentiation filter for even number data. *Signal Process.* 2005; 85:1429-1434. <https://doi.org/10.1016/J.SIGPRO.2005.02.002>
- [15] Lyons RG. Wprowadzenie do cyfrowego przetwarzania sygnałów (Introduction to digital signal processing). Communications and Connectivity Publishing House. Warsaw 2000.
- [16] Maćkowski J, Wilk A. Analiza wywiązywania się ciepła jako podstawa projektowania procesu spalania w silniku (Heat release analysis as a basis for engine combustion design). *Czasopismo Techniczne.* 2008;105(7):105-114.
- [17] Molenda J, Charchalis A. Preliminary research of possibility of using thermovision for diagnosis and predictive maintenance of marine engines. *Journal of KONBiN.* 2019;49:49-64. <https://doi.org/10.2478/jok-2019-0050>
- [18] Optical pressure sensor. optrand.com (accessed on 3.07.2024).
- [19] Pandurangadu V, Reddy SSK. Theoretical investigations of injection pressure in a four stroke DI diesel engine with alcohol as fuel. *International Journal of Mechanical Engineering and Technology (IJMET).* 2013;4(2):209-216.
- [20] Pham VV. Research on the application of Diesel-RK in the calculation and evaluation of technical and economic criteria of marine diesel engines using the unified ULSD and biodiesel blended fuel. *Journal of Mechanical Engineering Research and Developments.* 2019;42:87-97. <https://doi.org/10.26480/jmerd.02.2019.87.97>
- [21] Pietras D, Sobieszkański M. Identification of numerical model and computer program of SI engine with EGR. *Journal of KONES Internal Combustion Engines.* 2003;10(1-2):197-204.
- [22] Pressure sensor data. gms-instruments.com/product/premet-m/ (accessed on 11.07.2024).
- [23] Puzdrowska P. Analiza informacyjności diagnostycznej temperatury spalin wylotowych okrętowego tłokowego silnika spalinowego (Diagnostic information analysis of exhaust gas temperature of a marine piston internal combustion engine). PhD dissertation. Gdansk University of Technology. Gdansk 2023.
- [24] Puzdrowska P. Diagnostic information analysis of quickly changing temperature of exhaust gas from marine diesel engine. Part I: single factor analysis. *Pol Marit Res.* 2021;28:97-106. <https://doi.org/10.2478/pomr-2021-0052>
- [25] Puzdrowska P. Metoda wyznaczania stałej czasowej termopary na podstawie pomiaru szybkozmiennej temperatury spalin wylotowych silnika o ZS (A method for determining the time constant of a thermocouple based on the measurement of the rapidly varying temperature of the exhaust gas of a diesel engine). *Scientific Journals of the Naval Academy in Gdynia.* 2018;108:115-133.
- [26] Rudnicki J, Girtler J. Quantumness in diagnostics of marine internal combustion engines and other ship power plant machines. *Pol Marit Res.* 2023;30:110-119. <https://doi.org/10.2478/pomr-2023-0064>
- [27] Stelmasiak Z, Matyjasik M. Simulation of the combustion in a dual fuel engine with a divided pilot dose. *Combustion Engines.* 2012;151(4):43-54. <https://doi.org/10.19206/CE-117020>
- [28] Stepanenko D, Kneba Z, Rudnicki J. Numerical methodology for evaluation the combustion and emissions characteristics on WLTP in the light duty dual-fuel diesel vehicle. *Combustion Engines.* 2022;189:94-102. <https://doi.org/10.19206/CE-143334>
- [29] Śliwiński K. Wpływ tlenowego wzbogacania mieszanki na wskaźniki robocze i ekologiczne silników o zapłonie iskrowym (The effect of oxyfuel mixture enrichment on the operating and environmental ratings of spark-ignition engines). Cracow University of Technology Publishing House. Cracow 2013.
- [30] Taghizadeh-Alisaraei A, Mahdavian A. Fault detection of injectors in diesel engines using vibration time-frequency analysis. *Appl Acoust.* 2019;143:48-58. <https://doi.org/10.1016/j.apacoust.2018.09.002>
- [31] Teodorczyk A, Rychter T. Teoria silników tłokowych (Theory of reciprocating engines). Communication and Connectivity Publishing House. Warsaw 2006.
- [32] Thermal camera data. avio.co.jp (accessed on 3.07.2024).
- [33] Thermocouples data. termo-precyzja.com.pl (accessed on 3.07.2024).
- [34] Varbanets R, Shumylo O, Marchenko A, Minchev D, Kyrnats V, Zalozh V et al. Concept of vibroacoustic diagnostics of the fuel injection and electronic cylinder lubrication systems of marine diesel engines. *Pol Marit Res.* 2022;29:88-96. <https://doi.org/10.2478/pomr-2022-0046>
- [35] Wang G, Zhou Y, Zhang Q, Wang S. The small sample failure distribution model of diesel engine component parts using FMECA approach. *International Journal of Modeling and Optimization.* 2017;7(1):19-23.
- [36] Wisłocki K. Studium wykorzystania badań optycznych do analizy procesów wtrysku i spalania w silnikach o zapłonie samoczynnym (A study of the use of optical testing for the analysis of injection and combustion processes in compression ignition engines). Habilitation dissertation. Poznan University of Technology Publishing House. Poznan 2004.
- [37] Wiśniewski S. Termodynamika techniczna (Technical thermodynamics). Scientific and Technical Publishing House. Warsaw 2022.
- [38] Witkowski K. Stan diagnostyki technicznej okrętowych silników tłokowych (The state of technical diagnostics of marine diesel engines). *Diagnostics.* 2005;34:85-92.
- [39] Wysocki J, Witkowski K. Increasing the efficiency of marine engine parametric diagnostics based on analyses of indicator diagrams and heat-release characteristics. *Energies.* 2023;16(17):6240. <https://doi.org/10.3390/en16176240>
- [40] Zacharewicz M, Kniaziewicz T. Research on energetic processes in a marine diesel engine driving a synchronous generator for diagnostic purposes. Part 2 – mathematical model of the processes. *Journal of Polish CIMEEAC.* 2016; 11(1):199-209.
- [41] Zacharewicz M. Metoda diagnozowania przestrzeni roboczych silnika okrętowego na podstawie parametrów gazodynamicznych w kanale zasilającym turbosprężarkę (A method for diagnosing the working spaces of a marine engine on the basis of gas-dynamic parameters in the feed channel of a turbocharger). PhD dissertation. Naval Academy. Gdansk 2009.

Patrycja Puzdrowska, DEng. – Faculty of Mechanical Engineering and Ship Technology, Gdansk University of Technology, Poland.
e-mail: patpuzdr@pg.edu.pl

